


ORIGINAL ARTICLE

Voluntary Wheel Running Exercise Evoked by Food-Restriction Stress Exacerbates Weight Loss of Adolescent Female Rats But Also Promotes Resilience by Enhancing GABAergic Inhibition of Pyramidal Neurons in the Dorsal Hippocampus

Tara G. Chowdhury¹, Gauri S. Wable¹, Yi-Wen Chen¹, Kei Tateyama¹, Irene Yu¹, Jia-Yi Wang¹, Alex D. Reyes¹ and Chiye Aoki ^{1,2}

¹Center for Neural Science, NYU, New York, NY 10003, USA and ²The Neuroscience Institute, NYU Langone Medical Center, New York, NY 10016, USA

Address correspondence to Chiye Aoki, Center for Neural Science, 4 Washington Place, New York, NY 10003, USA. Email: ca3@nyu.edu  orcid.org/0000-0003-4010-9425

Abstract

Adolescence is marked by increased vulnerability to mental disorders and maladaptive behaviors, including anorexia nervosa. Food-restriction (FR) stress evokes foraging, which translates to increased wheel running exercise (EX) for caged rodents, a maladaptive behavior, since it does not improve food access and exacerbates weight loss. While almost all adolescent rodents increase EX following FR, some then become resilient by suppressing EX by the second–fourth FR day, which minimizes weight loss. We asked whether GABAergic plasticity in the hippocampus may underlie this gain in resilience. *In vitro* slice physiology revealed doubling of pyramidal neurons' GABA response in the dorsal hippocampus of food-restricted animals with wheel access (FR + EX for 4 days), but without increase of mIPSC amplitudes. mIPSC frequency increased by 46%, but electron microscopy revealed no increase in axosomatic GABAergic synapse number onto pyramidal cells and only a modest increase (26%) of GABAergic synapse lengths. These changes suggest increase of vesicular release probability and extrasynaptic GABA_A receptors and unsilencing of GABAergic synapses. GABAergic synapse lengths correlated with individual's suppression of wheel running and weight loss. These analyses indicate that EX can have dual roles—exacerbate weight loss but also promote resilience to some by dampening hippocampal excitability.

Key words: exercise, food restriction, glutamic acid decarboxylase, mIPSC, electron microscopy

Introduction

Adolescence is period of perfect storm (Casey et al. 2010), manifested as gains in cognitive function but also of the emergence of many mental disorders and maladaptive behaviors for the first time (Spear 2000). This may be because maturation of key brain structures underlying emotional processing and decision

making continues into adolescence (Mills et al. 2014; Chowdhury, Barbarich-Marsteller et al. 2014; Casey and Lee 2015; Saul et al. 2015), while exposure to novel environmental stressors is increased (Romeo 2010) as individuals travel farther away from their nest. We investigated the cellular and molecular mechanisms underlying adolescent female rats' individual

differences in vulnerability/resilience to food restriction (FR)-stress following acclimation to a running wheel in the cage (FR + EX). FR + EX captures important hallmarks of anorexia nervosa (AN): comorbidity of heightened anxiety (Chen, Surgent et al. 2017), chemical signatures of stress (elevated cortisol levels (Kinzig and Hargrave 2010)), excessive exercise (EX) (Wable, Min et al. 2015) plus voluntary FR (Chen et al. 2016), leading to >20% body weight loss within 3–4 days. Like the human condition of AN, FR + EX can be lethal, requiring rats to be removed from the FR + EX environment when weight loss exceeds 25%. Regarding the last point, adolescent rodents (mice and rats) that are acclimated to a running wheel become incessant runners within 24 h of imposed FR. The prevalence of the incessant running (~80%) may be because this is an innate behavior simulating foraging, a behavior that is adaptive for hungry animals in the wild but maladaptive to those in cages. Many individuals continue running, rather than eat, even during the hours of food availability. This combination of voluntary FR with excessive EX is what exacerbates the animals' weight loss to a point of lethality. In this way, FR + EX captures some of the features of the human condition of AN and is widely referred to as activity-based anorexia (ABA).

We view the ABA paradigm (i.e., FR + EX) as an animal model that enables us to understand the cell biological underpinnings of maladaptive behaviors, such as AN, as well as plasticity that converts maladaptive innate behaviors to more adaptive behaviors. This is because ABA also captures the attainment of resilience against the maladaptive behavior, measured among a subpopulation of animals as suppression of hyperactivity and minimized weight loss. For some individuals, suppression of food restriction-evoked hyperactivity is measurable as early as the second day of food restriction. For others, suppression of hyperactivity is measurable by the end of the first induction of ABA (fourth day) (Aoki et al. 1998; Aoki, Chowdhury et al. 2017) or only following a second ABA induction (Wable, Chen et al. 2015). Yet others continue to be hyperactive at all times, making them lose body weight the most (Chowdhury et al. 2013; Wable, Chen et al. 2015; Chen et al. 2016). The accompanying electron microscopic (EM) analysis revealed that the hippocampus and prefrontal cortex of resilient individuals had increased GABAergic innervation of pyramidal cells, while pyramidal neurons of those that remained hyperactive exhibited GABAergic innervations that were no different from naïve controls' (Chowdhury et al. 2013; Chen et al. 2016). In parallel studies, we showed that the hippocampus of resilient individuals also exhibit elevated levels of $\alpha 4$ and δ subunits of GABA_A receptors (GABA_ARs) extrasynaptically. EM revealed that these extrasynaptic GABA_ARs begin to rise within dendritic spines of hippocampal pyramidal neurons within 2 days (Aoki et al. 2014), become localized to excitatory synapses at spine heads within 4 days (Aoki et al. 2012; Aoki, Chowdhury et al. 2017) and persist at excitatory synapses through 2 rounds of ABA (Wable, Chen et al. 2015), where they are optimally situated to negatively modulate excitatory synapses through shunting inhibition (Shen et al. 2007, 2010). These findings support the idea that increased GABA responsiveness may contribute to reduced excitability of dorsal hippocampal pyramidal neurons which, in turn, contributes towards increased resilience to ABA.

In this study, we asked whether these changes that are suggestive of increased GABAergic modulation of dorsal hippocampal pyramidal neurons of adolescent rodents are paralleled by electrophysiologically measurable increases in GABA responsiveness and whether these changes can occur by the end of

the first ABA induction, that is, in time to confer resilience to a second ABA induction. We also asked whether changes evoked by ABA induction are due to exercise alone (EX), food restriction alone (FR) or might require their combination. To this end, we examined GABAergic responses following one ABA induction and compared these to controls that experienced EX or FR. A third group of control animals (CON) experienced neither FR nor wheel access. Although some knowledge now exists regarding changes in GABA_ARs at extrasynaptic site evoked by the experience of ABA, there is yet no knowledge regarding GABAergic synapses and the source of GABA within these brains during the first ABA induction. $\alpha 4$ - and δ -containing GABA_ARs that are expressed at dendritic spines are believed to be activated by volume transmission, with GABA arising from remote release sites that create ambient GABA, estimated to be about 1 μ M (Nusser et al. 1998; Wei et al. 2003; Mangan et al. 2005). The most prevalent class of GABAergic interneurons in the cerebral cortex are the subclass containing parvalbumin. These GABAergic interneurons form axosomatic synapses onto pyramidal neurons (Packer and Yuste 2011) and have been shown to be protective of stress-associated spine losses (Chen, Lu et al. 2017). Thus, in a separate set of 4 groups of animals (i.e., ABA, FR, EX, CON), we assessed the extent of axosomatic GABAergic innervations of pyramidal neurons in the dorsal hippocampus by EM to ask the same questions addressed electrophysiologically. We used adolescent females as subjects for ABA, so as to mirror the most vulnerable human population of AN (Kaye et al. 2009; Boraska et al. 2014).

Materials and Methods

Animals

All procedures involving the use of animals were in accordance with the NIH Guide for the Care and Use of Laboratory Animals and also approved by the Institutional Animal Care and Use Committee of New York University (Animal Welfare Assurance No. A3317-01). All animals were female Sprague-Dawley rats, purchased from Taconic Farms and shipped to New York University at the age of P28. All animals were housed in a room with a 12:12 light–dark cycle.

Rearing Conditions

The rearing conditions were nearly identical to the description in previous publications (Aoki et al. 2012; Chen, Actor-Engel et al. 2017) and thus are described only briefly here. A total of 127 female rats of ages P28 were singly housed from P28, corresponding to the age at the time of arrival from Taconic Farms. Of these, 94 were allotted for electrophysiology and 32 were allotted for EM-immunocytochemistry (ICC).

Sixty of those allotted to electrophysiology were CON, derived from 5 cohorts, ranging in age from PN32 to 50, to assess ontogenetic changes in GABAergic responses of the dorsal hippocampus. Overall, 34 additional animals allotted to electrophysiology were randomly assigned to one of 3 rearing conditions—ABA ($N = 20$, from 5 cohorts), EX ($N = 7$, from 4 cohorts) or FR ($N = 7$, from 4 cohorts)—with the age of experimental day (ED) ranging from P35 to P38 and were monitored daily through the age of euthanasia 8–9 days later, when they were PN 43–46.

The 32 animals allotted to EM-ICC were distributed evenly across the 4 experimental groups: 8 for CON, 8 for ABA, 8 for EX, and 8 for FR. Of these, one animal of the FR group was eliminated from analysis, because it had lost body weight even prior to FR. Their behavior and body weight will not be reported

here, because those data were already presented in a previous publication (Nedelescu et al. 2017). The wheel running and body weight data reported here pertain to those animals allotted to the electrophysiology part of the study, only.

Voluntary Wheel Running Activity

Animals designated for the ABA ($N = 20$, from 5 cohorts) and EX ($N = 7$, from 4 cohorts) groups were placed in a new shoebox-style cage with free access to a home cage running wheel of inner diameter 35 cm and running circumference per revolution of 110 cm (Med Associates, ENV-046). Wheel activity was measured continuously with 1-min temporal resolution for 7–8 days. FR and CON animals were reared in the absence of a running wheel. Animals of the FR and CON groups were not moved to shoebox-style cages.

Food Restriction

For animals designated for the ABA and FR groups, food access was restricted to the first hour of each ED, starting on ED 5, corresponding to ages P39 to P42 and for 4 consecutive days, through ED 8. The amount of food available to ABA and FR animals during the hour of food access was unlimited. Thus, ABA animals were food-restricted for the last 4 out of the 8 days of wheel access. EX and CON animals were reared with ad libitum food for all days and hours of the experiment.

Daily Measurements

All animals were weighed daily, just before the beginning of the dark phase. The amount of food that they consumed was also measured daily. Wheel activity was recorded manually once per day, at the time of body weight measurement and also continuously, using the software/hardware of ENV-046 (Med Associates). All animals were euthanized at the beginning of ED9, to prepare hippocampal slices.

Slice Physiology

Methods were as described in Shen et al. (2007, 2010), except as noted below. Briefly, rats were decapitated without anesthesia and brains were dissected out in ice-cold ACSF containing (in mM): 7 NaCl, 75 sucrose, 26 NaHCO₃, 2.5 KCl, 7 MgCl₂, 1.2 NaH₂PO₄, 10 glucose, 0.5 CaCl₂. Coronal slices (300 μm thickness) were made using a Leica VT1200S vibrating microtome. Slices were maintained at 37° for 30 min and thereafter at room temperature before recording. Slices were transferred to the recording chamber and continuously perfused with ACSF (composition as above except for CaCl₂ adjusted to 2 mM; 50 μM kynurenic acid (Sigma #K3375) and 0.5 μM TTX (Tocris #1069) were added to isolate postsynaptic GABA currents). CA1 pyramidal cells were visualized using an Olympus BX-51WI DIC-infrared upright microscope, and recorded using whole cell patch clamp procedures in voltage clamp mode at 26–30°. Patch pipettes had resistances of 5–10 MΩ when filled with (in mM): 140 CsCl, 5 HEPES, 5 EGTA, 2 Mg-ATP, 0.5 CaCl₂, 0.5 Li-GTP (Sigma G5884), pH 7.2, 290 mOsm. A 5 mM QX-314 was also added to block voltage-gated Na⁺ channels. Under these conditions the reversal potential for Cl⁻ is ~ 0 mV. Cells were held at -60 mV, so that evoked or spontaneous GABAergic activity produced an inward current. The GABAergic nature of the current was verified by block with 120 μM SR95531 (gabazine, Tocris #1262). Recordings were made with a Dagan PC-ONE amplifier, low-pass filtered at 3 kHz and digitized at 8 kHz using an Instrutech ITC-18 A/D converter and custom-written Igor

software (Wavemetrics Corp.). Data collection commenced after baseline currents had stabilized (generally within 15 min of establishing whole-cell mode).

Tonic GABA currents were evoked by 3 min bath application of 0.1 mM GABA. A subset of cells was filled with 0.5% biocytin, fixed by immersion in 4% paraformaldehyde, and subsequently visualized by DAB-HRP histochemistry (Horikawa and Armstrong 1988) for confirmation of cell type and location.

Data analysis was done offline using Matlab (Mathworks, Inc.). For the analysis of ontogenetic changes of electrophysiological properties of CON slices, the electrophysiologist was not blind to the treatment condition. For the other treatment conditions, the electrophysiologist was blind to the treatment condition. Response to applied GABA was measured as the initial slope (rise from 0 to 30% of peak) of the evoked current. sIPSC analysis was performed on 30 s of continuous baseline recording from each neuron, using a custom event-detection algorithm. Briefly, the raw traces were deconvolved with a kernel of the form:

$$\alpha(t) = \frac{-(e^{-t/\tau_1} - e^{-t/\tau_2})}{\tau_1 - \tau_2};$$

τ_1 and τ_2 were chosen for best fit to a composite sIPSC based on a random subset of manually identified events, using nonlinear least-squares. Event times were located wherever the deconvolved signal exceeded a fixed threshold, which was chosen for best match to manually identified event times in the raw traces for a subset of the data; the threshold was held constant for all analyses. This excluded most events <5 pA. The amplitude of each event was also measured baseline-to-peak, and decay time constant was determined by fitting an exponential to the decaying component. Statistical significance was tested using 2-sample Kolmogorov–Smirnov tests, except as noted.

EM-ICC for Analyzing Axosomatic GABAergic Synapses Onto Pyramidal Neurons in the Dorsal Hippocampus

In order to determine whether the 4 rearing conditions altered GABAergic innervation pattern of pyramidal neurons, hippocampi from 8 animals each of ABA, FR, EX, and CON, were analyzed. The 8 animals per group were allotted from 2 cohorts. Details of the glutamic acid decarboxylase (GAD) ICC procedure are as described in previous publications (Sarro et al. 2008; Chowdhury et al. 2013; Chen et al. 2016; Chen, Surgent et al. 2017). Body weight and wheel running details of animals used for this GAD ICC have been described in 2 other studies (Nedelescu et al. 2017; Chen, Actor-Engel et al. 2017) and thus are not presented here, except to note that their data were nearly identical to the pattern observed for the animals used for the current electrophysiological experiments and presented in this article.

Tissue Preparation for ICC

All were female Sprague Dawley rats of the exact same age, PN28, at the time of arrival to the NYU animal facility. At P44, corresponding to the eighth day of wheel access of the EX and ABA groups and the fourth day of food restriction for the ABA and FR groups, animals were anesthetized using urethane (34%; 0.65–0.85 mL/185 g body weight) via intraperitoneal injection, then euthanized by transcardial perfusion with a fixative consisting of 4% paraformaldehyde in 0.1 M phosphate buffer (pH 7.4) over 10 min at a flow rate of 50 mL/min. After

decapitation, brains were quickly removed from the skull. Brains were prepared into 2 mm-thick coronal slabs with a razor blade, to enhance postperfusion fixation of inner brain structures. The following day, coronal sections were cut with at a thickness set at 50 μm , using a Leica VT1000M vibrating microtome (vibratome) (Leica Microsystems GmbH, Wetzlar, Germany). The 32 animals were perfused on 4 different days, spanning 2 months. Antigenicity of tissue was preserved by storing them as free-floating sections in PBS with sodium azide (0.05%) at 3 $^{\circ}\text{C}$.

EM-ICC Detection of GABAergic Axon Terminals

Tissue from all animals were processed synchronously for EM-ICC, so as to minimize variabilities arising from differences in reagent qualities, incubation time, temperature, etc. The rabbit anti-GAD antibody used in this study (Lot 2069924 of Millipore, Bellerica, MA, USA, catalog number AB411; hereafter referred to as anti-GAD) recognizes both the GAD65 and GAD67 isoforms. Up to 3 free-floating vibratome sections from each brain were suspended in multiwells filled with 1 mL of 0.01 M phosphate buffer (PB) containing 0.9% sodium chloride (0.01 M PBS, pH 7.4), 0.05% sodium azide to retard bacterial growth, anti-GAD (1:400) and 1% bovine serum albumin to reduce nonspecific immunolabeling. On the following day, the excess unbound primary antibodies were removed by thoroughly rinsing the tissue with 0.01 M PBS. Tissue sections were incubated with biotinylated goat antirabbit-IgG secondary antibody (Vector Laboratories, Burlingame, CA; 1:200) diluted in PBS containing 1% bovine serum albumin and 0.05% sodium azide for 4 h on a shaker at room temperature. Next, tissue sections were thoroughly rinsed in PBS and incubated in PBS containing biotinylated HRP-avidin complex (ABC Elite kit, Catalog # 6100, Vector Laboratories). The immunolabel was visualized by the HRP-DAB procedure, with 3,3'-diaminobenzidine HCl (DAB) and H_2O_2 as substrates. DAB solution was prepared by dissolving 1 DAB tablet (10 mg, Sigma #D-5905) in 43 mL PBS and adding 4.3 μL of 30% H_2O_2 . Tissue sections were incubated in the DAB solution for 10 min. The HRP reaction was terminated by rinsing tissue sections in PBS, then processed for EM. The start time and end time of each of the immunoreagent incubation periods and rinse periods were staggered by approximately ~3 s per tissue source, with the exchanges of all 32 tissues accomplished in <2 min. The duration of the incubations and rinses were equalized, since the same sequence was kept for all periods of incubation/rinses.

Tissue Processing for EM

Free-floating vibratome sections were postfixated using 2% glutaraldehyde in PBS for 10 min, then with 2% osmium tetroxide for 60 min and 1% uranyl acetate in 70% ethanol overnight, then infiltrated with plastic. Ultrathin sections spanning CA1 of dorsal hippocampus were collected on grids, then counterstained with Reynold's lead citrate.

Quantitative EM Analysis

The EM images were captured digitally, using a 1.2 megapixel Hamamatsu CCD camera from AMT (Boston, MA) from the JEOL 1200XL electron microscope. The extent of contact formed upon pyramidal cells of the hippocampus by GAD-immunoreactive axon terminals was quantified using NIH's software, Image J (version 1.46r), to measure plasma membrane lengths contacted and not contacted by GAD-immunoreactive axon terminals.

Axon terminals were identified to be GAD-immunoreactive based on the accumulation of the DAB reaction product in the cytoplasm, excluding the lumen of vesicles and mitochondria. These terminals were identified to be forming synapses based on the parallel alignment of the axonal plasma membrane with the apposing cell's plasma membrane (Peters et al. 1991). Axon terminals residing immediately adjacent to the plasma membrane but lacking the clear parallel alignment of the plasma membrane with that of apposing cell's plasma membrane were also included in the analysis, since GABA regulates neuronal excitability through nonsynaptic as well as synaptic mechanisms (Liang et al. 2004).

Only those cell bodies that could be identified to be of pyramidal cells were included in the analysis. Somatic profiles were identified to be of pyramidal cells, based on the absence of indentations along the nuclear membranes, homogeneous distribution of chromatin within the nucleoplasm (Feldman 1984; Schlander and Frotscher 1986) and absence of GAD-immunoreactivity in the cytoplasm. Large dendritic profiles containing Nissl bodies and the Golgi apparatus were recognized to be the most proximal portions of dendrites that are in transition between somata and dendrites (Peters et al. 1991): the plasma membrane in these transition zones were excluded from analysis, so as to minimize ambiguity of the "somata" versus "dendrite" classifications. Otherwise, all of the profiles identifiable to be somata of pyramidal neurons were included in the analysis, strictly in the order that they were encountered along the vibratome-section surfaces, where penetration by immunoreagents would be maximal.

The EM Sampling Procedure

Sampling of the synaptic neuropil of the hippocampal CA1 was designed to optimize immunodetection, while also maintaining randomness of sampling. The electron microscopist sampling the ultrathin section was kept blind to the animal's ante mortem behavioral characteristics. The sampling size from each animal was equalized to be 5 somatic profiles per animal, totaling 40 per group. The mean and standard errors of means (SEM) values were determined for each animal. The mean length of the GAD-immunoreactive axon terminals contacting somata, the mean number of GAD profiles per 10 somata and the mean percentage of the plasma membrane contacted by GAD terminals were also compared across the treatment groups.

Statistical Analyses

For data sets that passed the KS, Shapiro-Wilk and D'Agostino & Pearson omnibus normality tests, group comparisons used Student's unpaired t-test for comparing ABA versus CON. When comparing all 4 groups (ABA, FR, EX, CON), one-way ANOVA was performed, followed by Fisher's post hoc analysis. Two-way ANOVA was also performed, to determine the main effect of FR and wheel running, also followed by Fisher's post hoc analysis. For data sets that did not pass the normality test, the Mann-Whitney test was performed to compare ABA versus CON and the Kruskal-Wallis test was performed to compare all 4 groups, followed by the uncorrected Dunn's test. For EM analyses, outliers were identified, then excluded using Prism's ROUT method (Motulsky and Brown 2006) by setting the false discovery rate to 1%, assuming Gaussian distribution. Potential association between 2 measurements were assessed by the Pearson correlation analysis. For all analyses, $P < 0.05$ was accepted as significant and $P \leq 0.1$ but >0.05 were considered to be of marginal significance.

Results

FR Evokes Hyperactivity, Exacerbating Weight Loss

Overall, 34 female rats were allotted to the ABA ($N = 20$), EX ($N = 7$), or FR ($N = 7$) group. All of them exhibited increased body weight from ED 1 through ED 5, as is expected for adolescents of this age range (Fig. 1A). At the beginning of ED 5, when imposition of FR began, there was no group difference in body weights. Beginning on ED 5, ABA and FR groups began losing weight, while the EX group continued to gain weight up to the end of the experimental period. Within 24 h (beginning of ED 6), the difference in the group mean values of ABA's and EX's reached statistical significance ($t[27] = 3.214$; $P = 0.003$) and the group difference continued to increase in subsequent EDs ($t[26] = 5.239$; $P = 2 \times 10^{-5}$ at the beginning of ED 7; $t[24] = 7.897$; $P = 4 \times 10^{-8}$ by ED 8). By the beginning of ED 7, ABA group's average body weight also diverged from FR's ($t[23] = 2.353$; $P = 0.03$) and continued to diverge ($t[24] = 2.929$; $P = 0.007$) by the beginning of ED 8. This divergence in the body weight between the FR and ABA groups replicates our previous observation (Aoki, Chowdhury et al. 2017), indicating that voluntary wheel access contributed towards the exacerbated weight loss of the ABA group.

Indeed, analysis of voluntary wheel running revealed that this activity was augmented greatly by food restriction (Fig. 1B). Six out of the 7 adolescent female rats assigned to the EX group and 20 of the 20 rats assigned to the ABA group exhibited increases in wheel running from ED 1 to the end of the EDs. Those designated to the EX group exhibited steady increases in the daily wheel running, reaching a group average rate of 1.93 ± 0.61 km/24 h by ED 7, which represented tripling in the daily

running rate relative to ED 1, when they were exposed to the wheel for the first time. In comparison, wheel running by the ABA group exhibited a particularly sharp rise within 24 h of food restriction, jumping from 1.59 km/day to 2.85 km/day by the beginning of ED 6. The group difference reached statistical significance by the beginning of ED 7 (5.74 km/day for the ABA group, 1.94 km/day for the EX group; $t[24] = 2.24$, $P = 0.03$) and continued to increase to 7.14 ± 1.23 km/24 h by the beginning of ED 8.

Correlation analysis revealed that maximum wheel activity correlated positively with the animal's maturity, reflected by their body weights on ED 5, just before FR began ($r = 0.23$; $P = 0.04$) (Fig. 1C). In contrast, the loss of body weight associated with the imposition of FR for 4 days correlated strongly and negatively with FR-evoked hyperactivity (Fig. 1D,E), indicating that the greatest amount of body weight was lost by subjects that exhibited the greatest hyperactivity.

GABA-Evoked Current is Unchanged During Midadolescence of CONs but is Augmented by ABA

Adolescence is a period of robust growth for hippocampal pyramidal neurons, with dendritic arbors doubling in complexity between P32 and P50 (Chowdhury, Rios et al. 2014; Bekhbat and Neigh 2018). This increase in dendritic branching occurs without decrease in spine density, indicating that the number of sites for excitatory synaptic inputs onto hippocampal neurons is also doubling. The current study aimed to determine whether this increase in dendritic arbor complexity and excitatory inputs is accompanied by changes in GABAergic

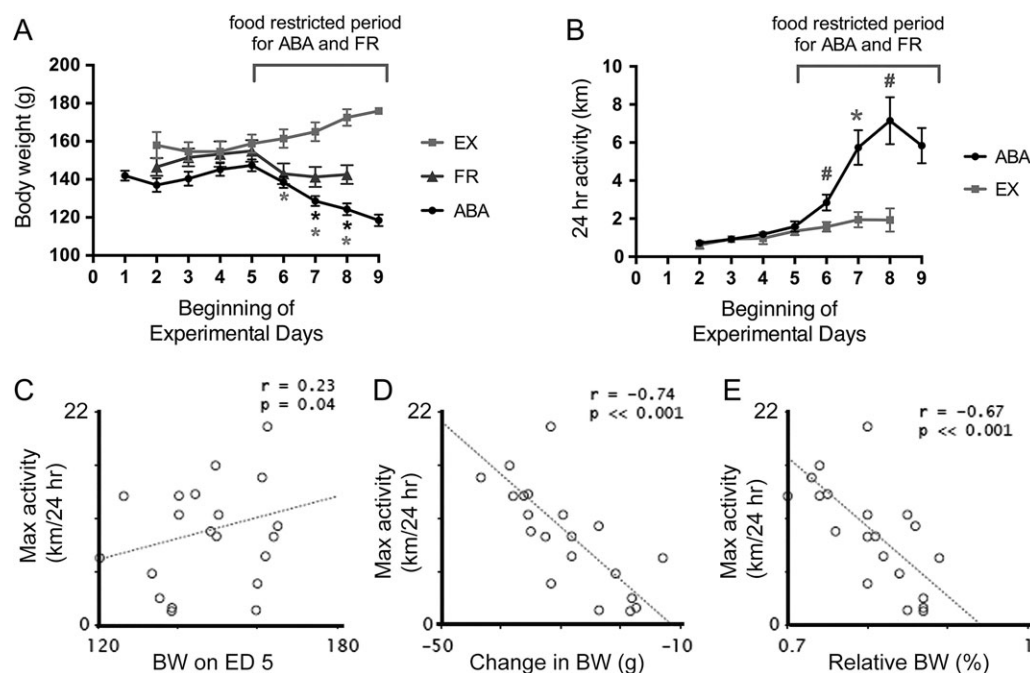


Figure 1. Body weights and wheel activity of ABA, FR, and EX groups of animals. (A) ABA animals exhibited significantly greater weight loss than FR and EX in the postnatal (PN) 32–50 age group, within 24 h of food restriction, measured at the beginning of ED 6 and through ED 8. ED 9 corresponds to the day of electrophysiological recordings. (B) Wheel activity of ABA animals became significantly greater than EX group's, beginning on ED 5, which corresponds to the first 24 h after the restricted food access schedule had begun. Hyperactivity persisted through the last full day of wheel activity, ED 8. (C) Pearson correlation analysis indicated that body weight of the animals at the beginning of the food-restricted period (ED 5) correlates weakly and positively with the animals' subsequent maximum wheel activity. (D and E) In contrast, the same animals' maximum wheel activity per 24 h of ABA animals correlated strongly and negatively with changes in body weight resulting from food restriction, relative to ED 5 (⇒just prior to the commencement of the food-restriction period), whether measuring the body weight change in grams (D) or as a percent of the body weight on ED 5 (E). Light asterisks indicate significant differences between the averaged values of the ABA group and EX group, while dark asterisks indicate significant differences between the averaged values of the ABA group and FR group. #Marginally significant differences ($0.1 \geq P > 0.05$).

inhibition. To address this question, inward currents evoked upon hippocampal pyramidal neurons by the application of GABA was measured, using whole cell patch clamp procedures, with cells held at -60 mV and with the reversal potential for Cl^- at ~ 0 mV (Fig. 2A). GABA responses of hippocampal pyramidal neurons were measured as the initial slope (rise from 0 to 30% peak) of the evoked current. Analysis of neurons sampled from the hippocampus of CON animals showed no age-related change ($r = -0.35$; $P = 0.09$, with 1 outlier excluded from the analysis) (Fig. 2B).

Using the same condition for whole-cell recording, we compared the GABA responses of hippocampal pyramidal neurons from rats that had undergone the experience of ABA, relative to the GABA responses of CON animals of the age range P40–49. For group comparisons of GABA-evoked responses, values > 14 pA/s were considered outliers and excluded. There were 2 such values for the ABA group and 1 for the CON group. Pyramidal neurons from the hippocampus of ABA animals, ranging in age from PN 43 to 46 (1.12 ± 0.23 pA/s (mean \pm SEM), $n = 18$ neurons from 10 animals), exhibited greater GABA-evoked current than of CON's (0.47 ± 0.15 pA/s, $n = 11$ neurons from 9 animals). This difference was significant by the Mann Whitney test ($P = 0.01$, 2-tailed, Fig. 2C). When outliers were kept, the difference was still significant ($P = 0.01$, $n = 12$ neurons for CON, $n = 20$ neurons for ABA).

We next asked whether GABA response could be augmented by FR alone or by EX alone. Kruskal–Wallis test indicated a significant difference among the 4 groups ($\chi^2(3) = 7.851$; $P = 0.049$). The mean GABA responses for the FR group (0.75 ± 0.16 pA/s, $n = 30$ neurons from 7 animals) and the EX group (0.62 ± 0.13 pA/s, $n = 27$ neurons from 7 animals) were similar to CON group's ($P = 0.41$ and 0.44 for comparisons of FR and EX groups, respectively). ABA group's values were significantly different than EX group's ($P = 0.03$) and FR group's values ($P = 0.03$, Fig. 2C). There were no outliers among the EX or FR groups.

Miniature Inhibitory Postsynaptic Currents are Altered by ABA, FR, and EX

Spontaneous miniature inhibitory postsynaptic currents (mIPSCs), such as those shown in Figure 3A, were analyzed to assess the prevalence of GABAergic synapses on pyramidal neurons of the dorsal hippocampus. Traces from ABA rats (29 neurons, 7763 events) did not differ markedly from CON's (17 neurons, 3564 events) but empirical CDFs (cumulative distribution frequencies) revealed a left-ward shift for both the amplitude (Fig. 3B) and interevent interval (Fig. 3C) of mIPSCs for the ABA tissue, indicating subtle decreases in amplitude, accompanied by increased frequency of mIPSC events.

Further comparison across all 4 groups by one-way ANOVA revealed a significant group difference in mIPSC amplitudes ($F[3,85] = 11.72$, $P < 0.0001$). Post hoc analysis revealed that ABA rats' mean mIPSC amplitudes (14.34 ± 0.98 , $n = 29$ neurons from 12 animals) differed significantly from EX's (9.35 ± 0.54 , $n = 24$ neurons from 7 animals, $P = 0.0002$) and also from FR's (9.97 ± 0.79 , $n = 19$ neurons from 6 animals, $P = 0.002$), and that the decrease in amplitude relative to CON's (16.81 ± 1.63 , $n = 17$ neurons from 7 animals) that was detected by CDF was marginally significant ($P = 0.09$, 80% Power, Fig. 3D). FR and EX groups' mean mIPSC amplitudes were also significantly reduced, compared with CON's ($P < 0.0001$ for both). Two-way ANOVA revealed no significant main effect of FR and only a weak main effect of EX ($P = 0.13$) but a highly significant interaction of the 2 ($F[1,85] = 33.90$, $P < 0.0001$).

mIPSC frequency from ABA tissue (9.90 ± 0.93 , $n = 29/N = 12$) increased significantly, relative to CON's (6.85 ± 0.87 mean \pm SEM, $n = 17$ neurons from 7 animals, $P = 0.02$), thereby corroborating the CDF analysis. One-way ANOVA of the 4 groups indicated a significant difference ($F[3,84] = 4.031$, $P = 0.01$). Post hoc analysis revealed that mIPSC frequency of the ABA group was significantly greater than FR's (6.1 ± 0.86 , $n = 19/N = 6$, $P = 0.002$) and marginally greater than EX's (7.57 ± 0.95 , $n = 24$ neurons from 7 animals, $P = 0.03$) (Fig. 3D). Two-way ANOVA revealed no main effect of FR but a main effect of the wheel's presence ($F[1,85] = 5.590$, $P = 0.02$) and no significant interaction of the 2 factors.

The mIPSC decay constant, tau, of ABA tissue (25.61 ± 1.31 , $n = 29$ neurons from 12 animals) differed significantly from CON's (21.52 ± 0.89 , $n = 17$ neurons from 7 animals, $P = 0.02$). One-way ANOVA indicated a significant difference among the 4 groups ($F[3,85] = 0.0025$). Post hoc analysis revealed that although CON's values also differed significantly from FR's (27.6 ± 1.59 , $n = 19$ neurons from 6 animals, $P = 0.002$) and EX's (28.06 ± 1.05 , $n = 24$ neurons from 7 animals, $P = 0.001$), ABA's values did not differ from FR's ($P = 0.24$ for ABA vs. FR) and ABA's values differed only marginally from EX's ($P = 0.12$, 30% Power). Two-way ANOVA revealed marginal main effects of the wheel ($P = 0.07$) and of FR ($P = 0.14$) and a stronger interaction of the wheel and FR effects ($F[1,85] = 12.13$, $P = 0.001$).

EM-ICC Measurements of GABAergic Innervation of Pyramidal Neurons in the Dorsal CA1

Might the increased frequency of mIPSC following ABA (Fig. 3D) reflect an increase in the number of GABAergic synapses formed on cell bodies of pyramidal neurons? Might the decreased amplitude of mIPSCs among the EX and FR animals reflect decreased GABAergic synapse sizes? Might the increased GABA-evoked current amplitude reflect an increase in the proportion of GABAergic synapses formed on the plasma membrane of cell bodies? In order to address these questions, we used EM-ICC to directly measure the number of GABAergic synapses encountered per unit length of the plasma membrane of pyramidal neurons, the mean lengths of GABAergic synapses formed on cell bodies, and the proportion of plasma membrane of the cell bodies with which GABAergic terminals form synapses (Fig. 4). GABAergic terminals were readily identified by the accumulation of diffuse HRP-DAB reaction products in the cytoplasm surrounding small clear vesicles and mitochondria, indicating immunoreactivity to GAD, the GABA-synthesizing enzyme. GAD axon terminals forming axosomatic synapses were typically sandwiched between astrocytic processes with irregular contours and translucent cytoplasm (red asterisks in Fig. 4).

Comparison of the mean number of GAD terminals per unit length of cell body plasma membrane revealed a significant effect of the rearing condition (Kruskal–Wallis test, $\chi^2[3] = 51.05$, $P < 0.0001$). Dunn's test for multiple comparisons (Fig. 4C) revealed a highly significant reduction for the FR group ($0.05 \pm 0.01/\mu\text{m}$, $P < 0.0001$, $n = 36$ neurons from 7 animals) and EX ($0.13 \pm 0.01/\mu\text{m}$, $n = 40$ from 8 animals, $P = 0.0003$), compared with CON ($0.24 \pm 0.02/\mu\text{m}$, $n = 40$ neurons from 8 animals). However, when the treatment of FR and voluntary wheel running were combined (i.e., ABA), the effect was weaker although still in the direction of reduction ($0.18 \pm 0.02/\mu\text{m}$; $n = 40$ neurons from 8 animals; $P = 0.07$, 50% Power), compared with CON. FR group's value departed greatly from all other groups ($P < 0.0001$ when compared with ABA; $P = 0.0008$ compared with EX).

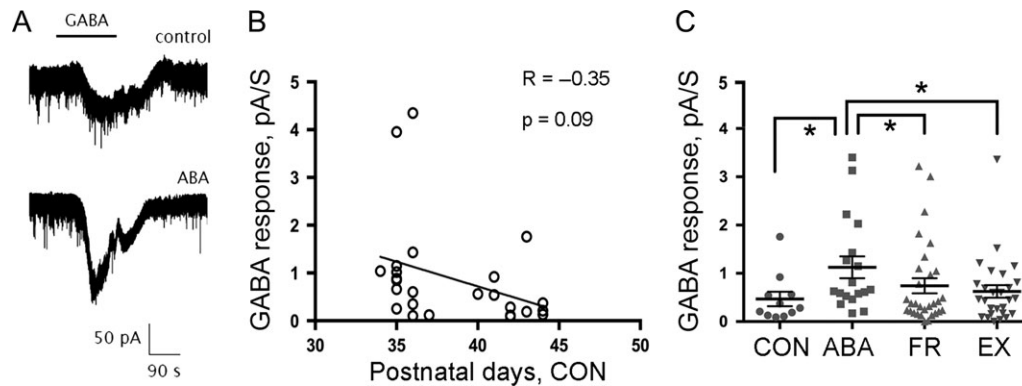


Figure 2. GABA current ontogeny in CA1 of the dorsal hippocampus of CON animals and the effect of ABA. GABA response of ages ranging from postnatal P34–P45 are shown. (A) A representative current trace following application of 0.1 mM GABA. (B) Initial slope of GABA responses of cells recorded from pyramidal neurons of CON animals (y-axis) for all cells at the postnatal days are indicated. There was a weak correlation between GABA response and postnatal ages. (C) Comparison of GABA responses of pyramidal neurons obtained from CON animals of PN 40–49 (0.47 ± 0.15 pA/s, mean \pm SEM, $n = 11/N = 9$ animals) and ABA animals of PN 43–46 (1.12 ± 0.23 pA/s, $n = 18/N = 10$) revealed a statistically significant difference ($P = 0.01$ by Mann–Whitney test, with or without the outliers). ABA's averaged GABA response was also significantly different from age-matched FR's (0.75 ± 0.16 pA/s, $n = 30/N = 7$, $P = 0.02$) and from age-matched EX's (0.62 ± 0.13 pA/s, $n = 27/N = 7$). * $P < 0.05$.

Interestingly, this pattern across the groups did not follow the prediction based in mIPSC frequency (Fig. 3D).

Comparison of the mean lengths of GAD terminals, averaged for each cell body also revealed a significant effect of the rearing condition (Kruskal–Wallis test, $\chi^2[3] = 16.65$, $P = 0.0008$). Dunn's multiple comparison analysis (Fig. 4D) revealed a highly significant increase for the FR group (0.98 ± 0.08 μ m, $P = 0.005$, $n = 28$ neurons from 7 animals), the EX group (1.08 ± 0.07 μ m, $P = 0.0001$, $n = 36$ neurons from 8 animals) and the ABA group that received a combination of food restriction and wheel access (0.92 ± 0.06 μ m, $P = 0.02$, $n = 35$ from 8 neurons), relative to CON group's values (0.73 ± 0.03 μ m, $n = 39/N = 8$) (Fig. 4D). This pattern across the groups also did not follow the prediction based on mIPSC amplitude (Fig. 3D). In fact, the pattern across the groups was the opposite of that for the mean mIPSC amplitudes.

The opposing effects comprised of axon terminal enlargement and axon number reduction yielded no net change in the percent of pyramidal cell body plasma membrane lengths forming synapses with GABAergic terminals within ABA brains ($15.5 \pm 1.5\%$, $n = 40$ neurons from 8 animals) compared with CON ($17.3 \pm 1.5\%$, $P = 0.38$, $n = 40$ neurons from 8 animals) but the extent of innervation by GABAergic terminals was greatly reduced for the FR group (5.9 ± 1.1 , $n = 38$ neurons from 7 animals, $P < 0.0001$) and marginally for the EX group (13.7 ± 1.7 , $P = 0.07$, $n = 40$ neurons from 8 animals) (Kruskal–Wallis test $\chi^2[3] = 31.44$, $P < 0.0001$) (Fig. 4E).

The cohort of ABA animals that underwent GAD analysis exhibited individual differences in the extent of weight loss, ranging from 11% to 23%, relative to baseline just before food restriction began on ED 5. This range of variance was as noted previously for another cohort of female rats that underwent the experience of ABA during adolescence (Aoki et al. 2012, 2014; Chowdhury, Barbarich-Marsteller et al. 2014; Chowdhury, Rios et al. 2014). We wondered whether individual differences of this measure of vulnerability to ABA were related to individual differences in GABAergic innervation of hippocampal pyramidal neurons, which varied by approximately 15% above and below the group mean value. Indeed, Pearson correlation analysis revealed a highly significant correlation between the mean lengths of synapses formed by GAD terminals onto pyramidal neurons of the hippocampus and the extent to which animals lost body weight. This correlation was highly significant, whether comparing GAD terminal lengths to each animal's body weight loss during the food-restricted periods (ED 5–ED 8),

relative to the body weight on ED 5, just before food restriction began ($R = 0.87$, $P = 0.01$) (Fig. 5A, left) or in grams of weight lost ($R = 0.84$, $P = 0.02$; Fig. 5B, left), or based on each animal's extent of weight loss on the last day of food restriction, ED 8 ($R = 0.78$, $P = 0.04$; Fig. 5C, left). The weight loss over the 4 food-restricted days also correlated marginally with the extent of cell body innervated by GAD terminals for the ABA animals ($R = 0.70$, $P = 0.05$; Fig. 5D, left). Although individual differences in the extent of weight loss was noted for the FR group as well, ranging from 11% to 19%, this individual difference did not correlate at all with the GABAergic innervation pattern (Fig. 5E–H, right column).

The extent of FR-stress evoked wheel running is another measure of vulnerability. We compared individual differences in the total distance run from ED 2 through ED 7, which ranged from 7 to 45 km among ABA rats, to individual differences in GAD terminal lengths. Pearson correlation revealed a correlation of these 2 measures, which approached significance for ABA animals ($R = 0.70$, $P = 0.08$; Fig. 6, left). In contrast, although the EX group exhibited a wide range of wheel running activity, ranging from 5 to 31 km over ED 2 through 7, this individual difference did not correlate with the GABAergic innervation pattern at all ($R = 0.04$, $P = 0.92$; Fig. 6, right).

Discussion

Does EX Promote Resilience Against Food Restriction Stress?

Whether exercise promotes resilience against food restriction is an important question that can be addressed by examining what features are altered for the ABA group, relative to those animals that experienced food restriction without exercise. GAD innervation of the hippocampus (Fig. 4C,E) was greater for ABA and EX, relative to food restriction. mIPSC amplitude and frequency were also greater for the ABA animals, compared with FR. We think this pattern supports the idea that exercise promotes resilience through plasticity of the GABAergic system in the dorsal hippocampus, particularly since increased GABAergic inhibition of the dorsal hippocampus is known to be anxiolytic (Huttunen and Myers 1986; Kataoka et al. 1991; Talaenko 1993). In contrast, animals that experienced food restriction without exercise also exhibited individual differences in vulnerability to this form of stress, quantified as the extent of weight loss, but

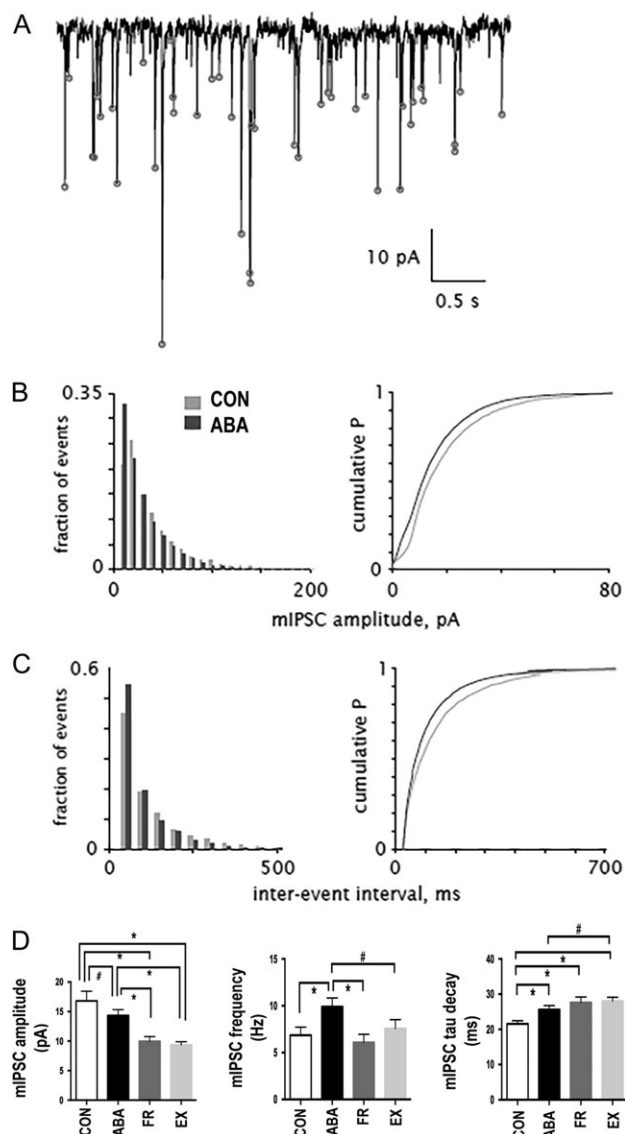


Figure 3. mIPSC comparisons of pyramidal neurons of CON, ABA, EX, and FR groups. (A) Example trace from the dorsal CA1 pyramidal neuron of a CON rat. Gray circles indicate peaks identified by the detection algorithm (see Materials and Methods). Traces from ABA rats were not different from CON traces by gross inspection, but showed quantitative differences (B–D). (B and C) left, histograms of mIPSC amplitudes (B) and interevent interval (C) for CON (light gray) and ABA (dark gray). Right, empirical CDFs of data. (D), pooled data on mIPSC amplitude (left), frequency (center), and decay time constant (right) from CON (white bars), FR (dark gray bars), EX (light gray bars), and ABA rats (black bars). Mean \pm SEM are shown.

without correlation with the extent of GABAergic innervation. This indicates that this aspect of the GABAergic system does not contribute to individual differences in vulnerability to FR, when EX is not part of the individual's experience.

In a previous study that analyzed dendritic branching of Golgi-stained neurons of the 4 groups, we observed retraction of dendritic branching and of the total lengths of dendrites spanning stratum radiatum of the dorsal hippocampus of both the EX and ABA groups (Chowdhury, Barbarich-Marsteller et al. 2014). Assuming no change in dendritic spines, this dendritic branch change, too, may dampen excitability of pyramidal neurons by reducing the potential sites for excitatory input.

Conversely, EX and ABA have both been shown to increase levels of NMDAR subunit NR2A-subunits at spines in stratum radiatum, while presynaptic and postsynaptic NR2B levels were increased by ABA and FR but not by EX (Chen, Actor-Engel et al. 2017). Moreover, those ABA individuals with the highest levels of postsynaptic NR2B exhibited the most severe weight loss. These findings indicate that exercise may promote resilience to food restriction-stress via changes in the GABAergic system, while stress associated with food restriction may exacerbate vulnerability to FR-stress by enhancing the glutamatergic system.

Presynaptic Mechanisms of Change at GABAergic Synapses Elicited by ABA

The electrophysiological data obtained following bath-application of GABA (Fig. 2) and analysis of spontaneous mIPSC (Fig. 3) indicate that ABA induces strengthening of GABAergic synapses through mechanisms that are presynaptic (increase in transmitter release probability or number of GABAergic axon terminals), postsynaptic (increase in the number of receptors or receptor current), and/or both. Here, we estimate the contribution of pre- versus postsynaptic mechanisms from these electrophysiological and anatomical (Fig. 4) data. We first describe our estimation of the contribution by presynaptic mechanisms.

The percent change in I_{GABA} amplitude following bath-application of GABA (Fig. 2), with ABA ($I_{GABA,ABA}$) above control ($I_{GABA,CON}$) is as follows:

$$\%change = 100(I_{GABA,ABA} - I_{GABA,CON})/I_{GABA,CON} = 138\%$$

I_{GABA} is approximated by:

$$I_{GABA} = aP_{pre}N_p$$

where a is the amplitude of a mIPSC, P_{pre} is the probability that the presynaptic terminal is active, and N_p is the number of synaptic sites on a single neuron, estimated based on EM data (Fig. 4C). Since synaptic sites are identified by EM, based on the direct juxtaposition of a presynaptic terminal with the postsynaptic specialization, $N_p = N_{pre} = N_{post}$. EM data indicated that $N_p, ABA = 0.75 N_{p,CON}$. When GABA is bath applied (Fig. 2), it is freely available to the postsynaptic receptors so that P_{pre} is effectively set to 1, masking any changes in the presynaptic release mechanisms. The data indicate changes in mIPSC amplitudes ($a_{ABA} = 14.34$ and $a_{CON} = 16.87$ for ABA and CON groups, respectively, from Fig. 3C). Based on these parameters, the percent change in I_{GABA} amplitude is actually predicted to decrease:

$$\begin{aligned} \%change &= 100(a_{ABA}P_{pre,ABA}N_p,ABA - a_{CON}P_{pre,CON}N_p,CON)/a_{CON}P_{pre,CON}N_p,CON \\ &= 100(a_{ABA}P_{pre,ABA}0.75N_p,CON - a_{CON}P_{pre,CON}N_p,CON) \\ &\quad / a_{CON}P_{pre,CON}N_p,CON \\ &= 100(a_{ABA}0.75 - a_{CON})/a_{CON} \\ &= 100(14.34(0.75) - 16.87)/16.87 = -36\% \end{aligned}$$

Not reflected in this calculation is the potential effects of the observed increase in mIPSC frequency, which may indicate an increase in P_{pre} . The maximum contribution of presynaptic mechanisms may be estimated by assuming the extreme, albeit unrealistic, scenario that the bath applied GABA is completely ineffective postsynaptically but modulates P_{pre} . Taking the mIPSC frequency (f) to be approximately equal to the product of the number of presynaptic terminals (N_{pre}) and P_{pre} divided by observation time t ($f = P_{pre}N_{pre}/t$) gives $P_{pre}N_{pre} = ft$. f_{ABA} was determined to be 9.9, while f_{CON} was 6.85 (Fig. 3D).

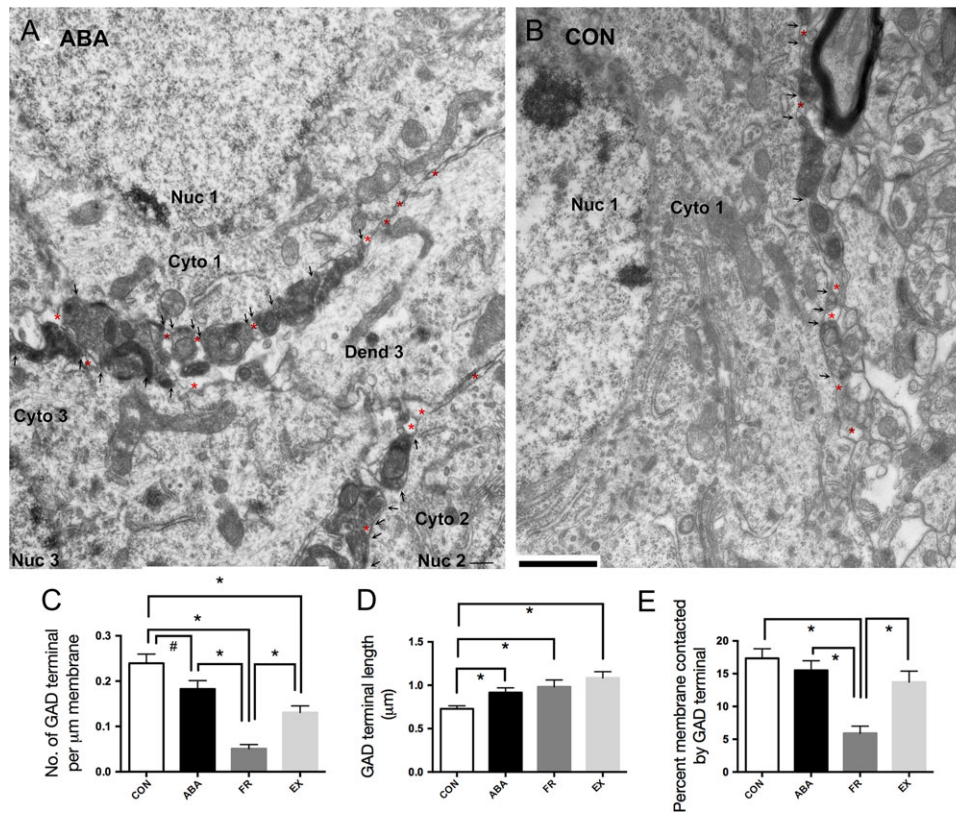


Figure 4. EM-ICC detection of the GABAergic marker, GAD, onto cell bodies of pyramidal neurons. GAD was detected using the HRP-DAB as the immunolabel. This approach revealed darkened puncta forming axosomatic synapses onto cell bodies in the PCL of the dorsal hippocampus. Arrows point to the lateral edges of GAD puncta, while red asterisks indicate portions of the plasma membrane that are contacted by astrocytic processes instead of GAD terminals. Such interdigitation of GAD terminals and astrocytes is evident along the cell body plasma membrane of neurons #1, #2, and #3 surrounding their cytoplasm “Cyto 1,” “Cyto 2,” and “Cyto 3”, respectively from the hippocampus of an ABA animal in panel A and from a CON animal in panel B. “Nuc” = nucleus of each cell. Bar = 1 μm . (C) The comparison of the mean number of GAD-immunoreactive terminals encountered per μm of plasma membrane length. This value was not significantly different between ABA and CON, although ABA’s value differed significantly from FR’s. (D) The group mean values of GAD terminal lengths encountered. The experience of ABA significantly augmented this value, relative to CON. (E) The percent of the plasma membrane contacted by GAD terminals. This value did not differ significantly between CON and ABA, but all groups’ values differed significantly from FR’s. All bars represent mean \pm SEM values. * $P < 0.05$; # $0.1 \geq P > 0.05$.

$$\begin{aligned}
 \% \text{change} &= 100(a_{\text{ABA}}P_{\text{pre,ABA}}N_{\text{p,ABA}} - a_{\text{CON}}P_{\text{pre,CON}}N_{\text{p,CON}})/a_{\text{CON}}P_{\text{pre,CON}}N_{\text{p,CON}} \\
 &= 100(a_{\text{ABA}}f_{\text{ABA}}t - a_{\text{CON}}f_{\text{CON}}t)/(a_{\text{CON}}f_{\text{CON}}t) \quad (if P_{\text{pre}}N_{\text{p}} = ft) \\
 &= 100(a_{\text{ABA}}f_{\text{ABA}} - a_{\text{CON}}f_{\text{CON}})/(a_{\text{CON}}f_{\text{CON}}) \\
 &= 100(14.34(9.9) - 16.87(6.85))/16.87(6.85) = 23\%
 \end{aligned}$$

The outcome of this calculation indicates that the increase in mIPSC frequency could account for 23% of the 138% increase in synaptic current that could be evoked through bath-applied GABA to activate postsynaptic receptors.

It is well known that wheel running induces increase of BDNF release in the hippocampus (reviewed in [Rendeiro and Rhodes \(2018\)](#)). BDNF-induced increase of docked vesicles increases spontaneous synaptic events, but, unlike what was observed for the ABA tissue, this is paralleled by increases in synapse number ([Tyler and Pozzo-Miller 2001](#)). Change in the vesicles dispersed randomly throughout the presynaptic terminal ([Rizzoli and Betz 2004](#)) or among the reserve pool ([Hirsch et al. 1999](#)) have also been ascribed to changes in mIPSC frequency and could have been induced by ABA.

Postsynaptic Mechanisms of Change at GABAergic Synapses Elicited by ABA

The difference between the measured (138%) and estimated change in $I_{\text{GABA,ABA}}$ based solely on presynaptic mechanisms

(23%) indicates an involvement of additional postsynaptic mechanisms that account for the remaining 115% of the increase. Below, we describe 2 possible types of postsynaptic mechanisms—the addition of extrasynaptic receptors and unsilencing of GABAergic synapses.

Addition of Extrasynaptic GABA_ARs

mIPSC amplitude analysis indicated a trend towards decrease for the ABA tissue, relative to CONs, yet responsiveness of pyramidal neurons to bath-applied GABA increased by much more (138%) following ABA. Although this discrepancy may be explained, in part, to the 50% increase in mIPSC frequency, we showed above that it is difficult to consider that this, alone, could account for the doubling in the magnitude of GABA-evoked response. We speculate that the addition of extrasynaptic GABA_ARs may also contribute to pyramidal neurons’ enhanced responsiveness to GABA (Fig. 7). Such a change is not expected to contribute to the measurement of mIPSC amplitude or mIPSC frequency. In support of this idea, the mIPSC decay constant is increased by ABA, relative to CON’s. The increased decay constant could be due to the combined kinetics of postsynaptic $\alpha 1$ -containing and a new population of peri-synaptic $\alpha 4$ -containing GABA_ARs that emerge within ABA tissue. Moreover, we have shown previously that the experience of

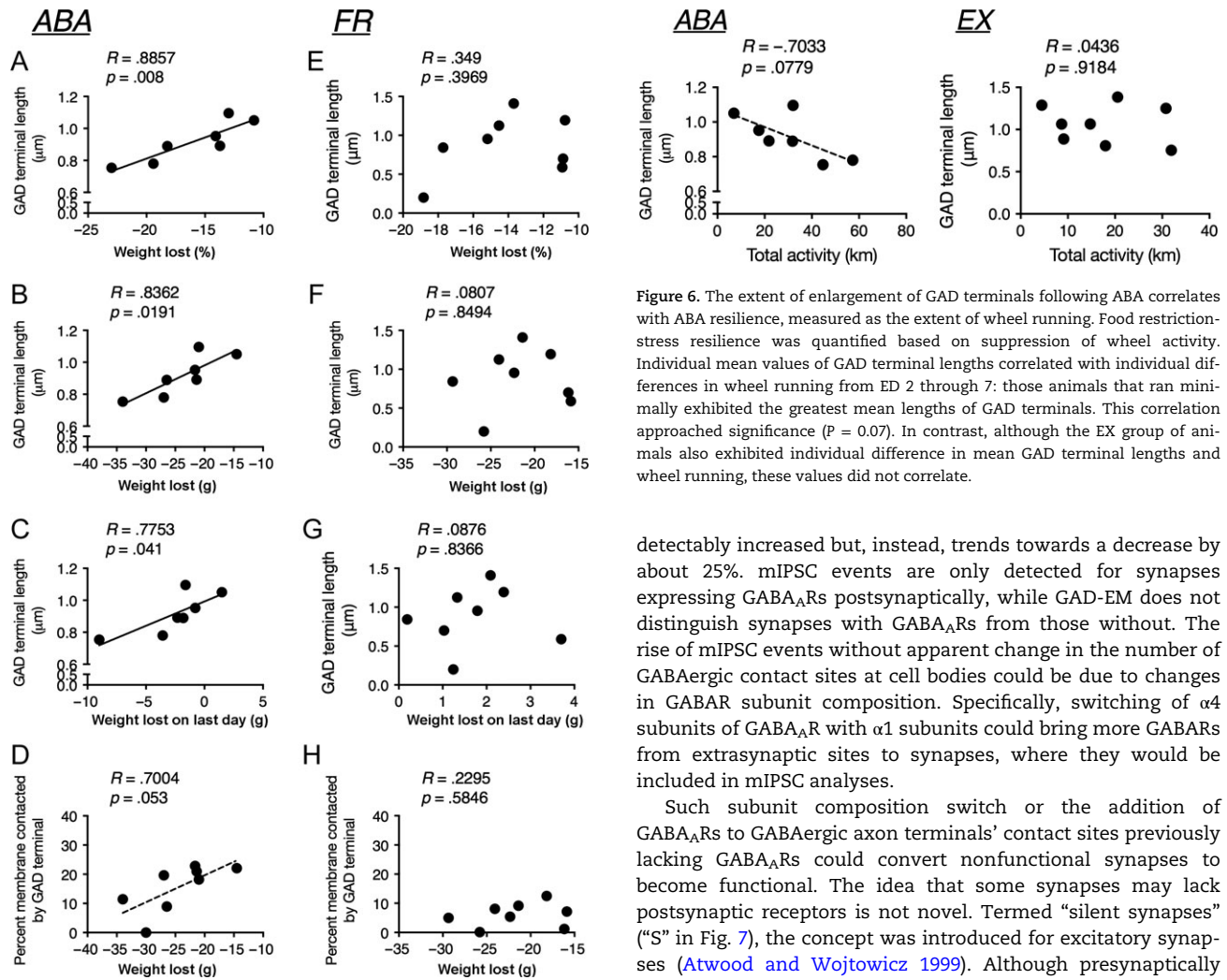


Figure 5. The extent of enlargement of GAD terminals following the experience of ABA correlates strongly with ABA resilience, measured as minimization of weight lost during the food-restricted days. ABA resilience was quantified as the minimalization of weight loss due to food restriction. The individual mean values of GAD terminal lengths varied by approximately 15% above and below the group mean value. These differences correlated significantly with individual differences in body weight lost, relative to the body weight on the day that food restriction began, which was ED 5 (A), or as absolute difference in grams of body weight lost (B), or the extent of body weight lost during the last day of food restriction, on ED 8 (C). Although the percent of plasma membrane contacted by GAD terminals did not differ between ABA and CON, individual differences in this value correlated somewhat with the weight lost during the 4 days of food restriction (D). Although animals that underwent food restriction without exercise (FR) also exhibited individual differences in weight loss, these values did not correlate with individual differences in GABAergic innervation (E–H).

ABA increases the expression of extrasynaptic $\alpha 4\delta$ -containing GABA_ARs, although this analysis was undertaken for dendrites in stratum radiatum, only, and not at cell bodies (Aoki et al. 2012, 2014; Aoki, Chen et al. 2017).

Unsilencing GABAergic Synapses

mIPSC frequency analysis revealed a significant increase induced by ABA, relative to CONs, yet direct observation of GAD innervations by EM indicated that the number of GAD terminals forming synapses onto pyramidal cell bodies is not

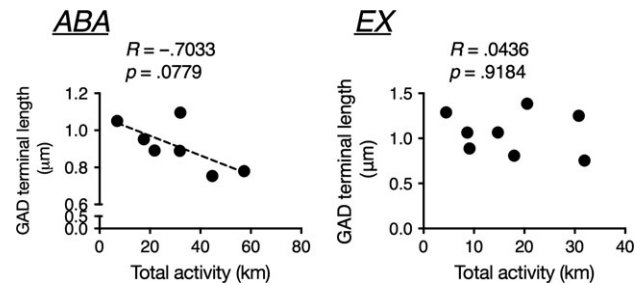


Figure 6. The extent of enlargement of GAD terminals following ABA correlates with ABA resilience, measured as the extent of wheel running. Food restriction-stress resilience was quantified based on suppression of wheel activity. Individual mean values of GAD terminal lengths correlated with individual differences in wheel running from ED 2 through 7: those animals that ran minimally exhibited the greatest mean lengths of GAD terminals. This correlation approached significance ($P = 0.07$). In contrast, although the EX group of animals also exhibited individual difference in mean GAD terminal lengths and wheel running, these values did not correlate.

detectably increased but, instead, trends towards a decrease by about 25%. mIPSC events are only detected for synapses expressing GABA_ARs postsynaptically, while GAD-EM does not distinguish synapses with GABA_ARs from those without. The rise of mIPSC events without apparent change in the number of GABAergic contact sites at cell bodies could be due to changes in GABAR subunit composition. Specifically, switching of $\alpha 4$ subunits of GABA_AR with $\alpha 1$ subunits could bring more GABARs from extrasynaptic sites to synapses, where they would be included in mIPSC analyses.

Such subunit composition switch or the addition of GABA_ARs to GABAergic axon terminals' contact sites previously lacking GABA_ARs could convert nonfunctional synapses to become functional. The idea that some synapses may lack postsynaptic receptors is not novel. Termed "silent synapses" ("S" in Fig. 7), the concept was introduced for excitatory synapses (Atwood and Wojtowicz 1999). Although presynaptically silent GABA synapses have been reported (Bekkers 2005), these are conceptually like the extrasynaptic GABARs. To the best of our knowledge, the existence of silent GABAergic synapses due to the absence of postsynaptic receptors is novel. We previously showed that apical dendrites of the ventral hippocampus of CON tissue undergo robust elaboration during adolescence, only to be pruned back by late adolescence (~P55) and that these changes are hastened by ABA induction (Chowdhury, Barbarich-Marsteller et al. 2014). It may be that unsilencing of GABAergic synapses is a maturational process also hastened by ABA, to take on characteristics resembling the state at P55. Studies are under way to assess the levels of GABA_ARs at axosomatic synapses of ABA versus CON tissue.

Contribution of GABAergic Synapses at Dendrites in the ABA-Induced Changes

We previously also showed that apical dendrites of pyramidal neurons in the dorsal hippocampus of mice undergo GABAergic synapse remodeling that are detectable following 2 ABA inductions: those individuals that are resilient, based on reduced hyperactivity, show greater percentage of apical dendrites innervated by GABAergic axon terminals, while those exhibiting hyperactivity that persists through both ABA inductions exhibit GABAergic innervation that is no different from CON's (Chowdhury et al. 2013). In another study that examined the hippocampus of mice after only one ABA induction during

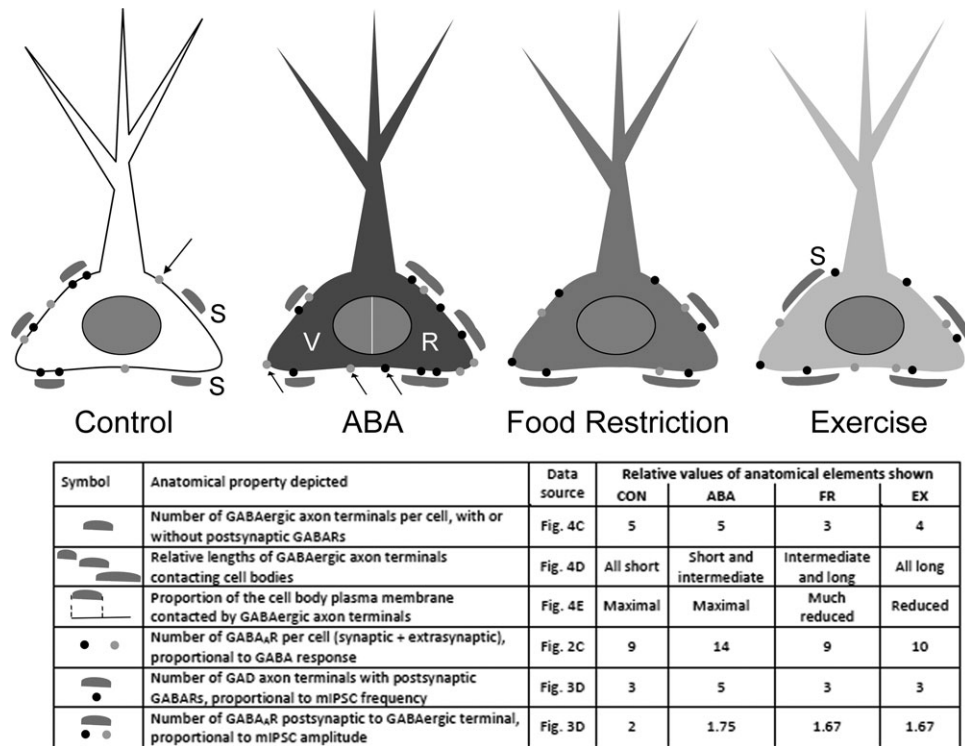


Figure 7. Summary of anatomical findings combined with electrophysiological data. Gray disks depict GABAergic axon terminals, while black and light gray dots depict GABA_AR clusters. Arrows point to extrasynaptic receptors, while S depicts silent synapses. EM revealed that food restriction and exercise both decrease the number of GABAergic axon terminals surrounding pyramidal cells, relative to control tissue but that the combination of the 2 treatments (ABA) does not decrease GABAergic axon number by as much (Fig. 4C). These changes are depicted by the number of disks surrounding the pyramidal cells of the 4 treatment groups. The changes in GABAergic terminal length (Fig. 4D) and percent of cell body plasma membrane contacted by GABAergic terminals (Fig. 4E) are also depicted with the disks. In spite of the slight decrease in GABAergic axon number within ABA brains, relative to Controls', mIPSC frequency is increased by ABA induction (Fig. 3D). The additional mechanism giving rise to the increase in mIPSC frequency could be a change in the proportion of GABAergic axon terminals facing GABA_AR clusters, rendering these contact sites fully functional (unsilenced). These fully functional GABAergic synapses are depicted by the number of disks surrounding pyramidal cell bodies that are matched by postsynaptic GABA_ARs. In contrast, those axon terminals that are not matched by GABA_ARs would be silent (S). Such unsilencing of GABAergic synapses following ABA induction fits with the increase in mIPSC frequency, in spite of the decrease in the number of GABAergic terminals. Electrophysiological data indicate that GABA-evoked response is augmented within ABA brains, even though the number of GABAergic axon terminals (Fig. 3C) and mIPSC amplitude (Fig. 2D) are decreased by ABA. Since mIPSCs only record synaptically located GABA_AR activity, the increase in GABA-evoked response may be due, in part, to the increase of extrasynaptic GABA_ARs (arrows pointing to dots on Control and ABA cells but also present for Food Restriction and Exercise cells). Extrasynaptic GABA_ARs are often comprised of distinct subunit compositions. This putative difference in subunit composition is depicted by the mixture of black and gray dots. mIPSC tau decay was significantly increased by food restriction alone, exercise alone and by the combination of the 2 treatments. This could be due to GABA_AR subunit switching, such as the $\alpha 4$ subunits that displace $\alpha 1$ subunits. This idea is also depicted by the admixing of gray (putatively $\alpha 4\beta 6$ -GABA_AR) and black (putatively $\alpha 1\beta \gamma$ -GABA_AR) dots. Individualized EM analyses (Figs 5 and 6) suggest that the resilient individuals ("R," right half of the ABA cell body) exhibit lengthened GABAergic terminals and greater percent contact onto pyramidal cell bodies, relative to the vulnerable ones (V in Fig. 7's ABA cell), which are anatomically more like Control cells.

adolescence but following a week of recovery showed that this experience was not sufficient to induce increases in GABAergic innervations of dendrites, relative to CONs (Chen, Surgent et al. 2017). It remains to be determined whether apical dendrites of adolescent rats exhibit increases in GABAergic synapses with pre- and postsynaptic specializations immediately after only one ABA induction, but we think this is unlikely, based on the observations described above. If ABA does evoke an increase in the number or size of GABAergic synapses along distal dendrites by the end of one ABA induction, this could also contribute to the increase in mIPSC frequency and GABA-evoked current.

The Effects of Food Restriction and Exercise in ABA are not Additive

FR alone and EX alone also reduced mIPSC amplitude, yet EM indicated that GAD terminals were lengthened for FR and EX animals. These opposite patterns suggest that FR and EX

promote growth of GABAergic terminals but without the concomitant increase of postsynaptic GABA_ARs. Matching this phenomenon, previous studies indicate that BDNF has a bimodal role for GABAergic innervation: it can promote development (Mizuno et al. 1994; Marty et al. 1996; Jiao et al. 2011) but also suppress GABAergic synaptic transmission, once the synapses are mature (Mizuno et al. 1994; Tanaka et al. 1997; Mizoguchi et al. 2003). It is possible that BDNF is the agent promoting both the lengthening of GABAergic axon terminals and removal of GABA_ARs postsynaptically within brains of FR and EX groups.

Although ABA combines food restriction with exercise, the effects of food restriction and exercise were neither additive nor synergistic in terms of mIPSC amplitude change. Instead, ABA minimized the reduction of mIPSC amplitude that was elicited by the FR and EX groups. Why ABA does not exhibit a pattern similar to FR and EX's remains a mystery. Similarly, although ABA increased mIPSC frequency, this effect was not detected in the FR or the EX group. Pyramidal neurons of FR and EX groups also exhibited no change in response to GABA

application, compared with CON's, even though their mIPSC amplitudes were significantly less than ABA's and CON's. This change, combined with the lengthened mIPSC decay constants of FR and EX groups, relative to CON's could reflect a switch in subunits of GABA_ARs at synapses from those containing $\alpha 1$ subunits (black dots in Fig. 7) (Goldstein et al. 2002) to other α -subunits (Eyre et al. 2012), including a $\alpha 4$ subunits (gray dots at synapses), which could increase responsiveness to bath-applied GABA, even with lower GABA_AR density per synapse (mIPSC amplitude data) by reducing receptor desensitization (Liang et al. 2004).

The Impact of GABAergic Plasticity on Behavior

The individualized EM analysis was able to reveal GABAergic synaptic changes correlating with individual differences in the suppression of wheel running and with minimized weight loss. Unfortunately, we could not assess correlation between electrophysiological data and individualized differences in the suppression of wheel running or weight loss. This is because our sampling from each brain that was allotted to electrophysiological analysis was limited to a few pyramidal cells. Based on our EM data, we have learned that a minimum of 5 cell bodies or 100 synapses per animal must be sampled before we obtain an averaged value that is representative of that brain region of that animal for then subjecting to correlational analysis with individualized behavioral or weight loss data.

Comparison of the averaged values of the ABA and CON groups revealed an increased GABA response (Fig. 2C) through increased expression of GABA_ARs (Aoki et al. 2014), together with increased GAD terminal lengths (Fig. 4D). These changes could augment vesicular release sites of GABA and dampen excitability of the hippocampus more. This may reduce anxiety-like behavior that drives excessive wheel running (Wable, Min et al. 2015), since hippocampus participates in anxiety regulation (Huttunen and Myers 1986; Kataoka et al. 1991; Talaenko 1993; Smith and Woolley 2004; Shen et al. 2007). Alternatively, since the correlation between GABAergic synapse length and body weight retention is greater than it is with wheel running, perhaps a more likely scenario is that boosting of GABAergic synapse strength somehow enables better weight retention in the face of FR, and the reduction of weight loss lessens the drive, in the form of anxiety and/or stress, to run on the wheel. In support of this idea, wheel running has been shown to be correlated tightly with anxiety that animals experience during FR (Wable, Min et al. 2015).

Although individual differences in the extent of weight loss was noted for the FR group, and the EX group exhibited a wide range of wheel running activity, these individual differences did not correlate with their GABAergic innervation pattern. Together, these findings indicate that the combination of food restriction stress and the opportunity to exercise voluntarily can both exacerbate weight loss but also promote GABAergic synapse plasticity. In another study that examined the behavioral responses of adolescent female mice to repeated FR, we noted that the proportion of individuals exhibiting ABA vulnerability dropped from 80% to 50% (Chowdhury et al. 2013). The present finding offers one mechanism underlying the gain of resilience—that is, enhanced GABAergic inhibition of the dorsal hippocampus—that occurs by the end of the first exposure to ABA and is likely to persist past weight restoration, thereby providing protection against a repeated exposure to the stress associated with FR.

Based on the connectivity of the hippocampus with polysensory cortical, thalamic and amygdaloid regions, the gain in resilience against FR stress during midadolescence may offer protection against other forms of stress subsequently. This is an important question for which research is underway. On the other hand, dampening of hippocampal excitability may also lead to negative consequences. In healthy individuals, the hippocampus provides negative feedback to the hypothalamus–pituitary–adrenal cortex (HPA) axis, thereby preventing HPA hyperactivity. Might GABAergic suppression of hippocampal excitability perturb the negative feedback of the HPA? Indeed, CRH-mRNA in amygdala and blood corticosterone levels are elevated in the bodies of adult animals that experienced ABA as adolescents (Kinzig and Hargrave 2010). The hippocampal negative feedback is impaired following mild chronic stress due, in part, to the up-regulation of the mineralocorticoid receptor-nNOS pathway, and this is associated with the generation of depressive-like behavior (Zhu et al. 2014). Although nNOS is expressed by GABAergic interneurons in the hippocampus, we have not observed depressive-like behavior in mice that have undergone 2 rounds of ABA (based on immobility time in the tail suspension test, unpublished observations). This difference in the link to depressive-like behavior could be due to the nature of stress, presence of wheel, among other factors. It would certainly be of value to examine the functional connectivity between the hippocampus and the HPA axis, which is a well-studied topic (McEwen et al. 2015) but not yet applied to the animal model of ABA.

Although our study focused on the dorsal hippocampus, many additional brain regions, including the ventral hippocampus, amygdala, prefrontal cortex, are likely to also undergo changes following ABA, since these brain regions undergo changes following other forms of stress. We have examined these additional brain areas anatomically (Wable et al. 2014; Chen et al. 2016; Aoki, Chen et al. 2017) but not electrophysiologically.

General Remarks

Although best effort was made to combine electrophysiology with EM analysis, we acknowledge that some of the observations that reached only trend levels may have been due to limited sampling. Conversely, effects that reached statistical significance, in spite of such limited sample sizes may represent particularly strong environmental effects. Neuronal activity, as assessed by cFos immunoreactivity in dentate gyrus of the dorsal hippocampus, correlates tightly with wheel running distance 90 min before euthanasia (reviewed in Rendeiro and Rhodes 2018). Whether pyramidal cells in the dorsal hippocampus also show such correlation remains to be determined. Future studies that examine neuronal activity in vivo would greatly enhance our understanding of the relationship between voluntary wheel running, weight retention and hippocampal excitability under conditions of stress.

All 4 groups of animals were reared in isolation. Thus, it is necessary that we interpret the environmental effects of FR and EX, alone or in combination, as being additive to the stress associated with social isolation. With this caveat in mind, our findings suggest the utility of pharmacological treatments targeting hippocampal GABA_ARs, including the extrasynaptic $\alpha 4$ -containing GABA_ARs that respond to ambient levels of GABA (Shen et al. 2007). Whether GABAergic plasticity of the type that we observed is specific to midadolescence or to the hippocampus are among many questions that remain to be studied.

Clinical Significance

AN is a mental illness with high mortality rate, surpassing that of depression (Sullivan 1995; Nielsen et al. 1998; Birmingham et al. 2005; Arcelus et al. 2011). The illness is also associated with life-long struggles, with relapses greater than 30% (Steinhausen 2002; Smink et al. 2013) and still without accepted pharmacological treatments. ABA is an animal model that captures AN's maladaptive behavioral hallmarks—excessive exercise plus voluntary food restriction—but also individual differences in resilience to the stress associated with food restriction and weight loss. Using adolescent female rats in this model, we uncovered plasticity in the GABAergic system of dorsal hippocampus only of rats exhibiting resilience, measured based on suppressed wheel running and suppressed weight loss that are evident by the fourth day of food restriction-stress. These findings provide clues regarding individual differences in stress resilience and therapeutic interventions to help vulnerable individuals.

Funding

The Klarman Foundation Grant Program in Eating Disorders Research to C.A. National Institutes of Health fundings were as follows: (R21MH091445-01, R21 MH105846, R01NS066019-01A1, R01NS047557-07A1, EY13079 and R25GM097634-01 to C.A., T32 MH019524 to G.S.W., UL1TR000038 to T.G.C. NYU's Research Challenge Fund to C.A. Fulbright Graduate Study Grant to Y.W.C.

Notes

We thank Clive Miranda and Alice Liu for their assistance with animal handling and Dr Hermina Nedelescu with her assistance with wheel running and body weight analyses. Most importantly, we thank Dr. Robert Levy for his contribution to data acquisition and analysis of electrophysiological data. *Conflict of Interest:* None declared.

References

- Aoki C, Chen Y-W, Chowdhury TG, Piper W. 2017. $\alpha 4\beta 6$ -GABA receptors in dorsal hippocampal CA1 of adolescent female rats traffic to the plasma membrane following voluntary exercise and contribute to protection of animals from activity-based anorexia through its location at excitatory synapses. *J Neurosci Res.* 96:1450–1466.
- Aoki C, Chowdhury TG, Wable GS, Chen YW. 2017. Synaptic changes in the hippocampus of adolescent female rodents associated with resilience to anxiety and suppression of food restriction-evoked hyperactivity in an animal model for anorexia nervosa. *Brain Res.* 1654:102–115.
- Aoki C, Sabaliauskas N, Chowdhury T, Min JY, Colacino AR, Laurino K, Barbarich-Marsteller NC. 2012. Adolescent female rats exhibiting activity-based anorexia express elevated levels of GABA(A) receptor alpha4 and delta subunits at the plasma membrane of hippocampal CA1 spines. *Synapse.* 66:391–407.
- Aoki C, Venkatesan C, Kurose H. 1998. Noradrenergic modulation of the prefrontal cortex as revealed by electron microscopic immunocytochemistry. *Adv Pharmacol.* 42:777–780.
- Aoki C, Wable G, Chowdhury TG, Sabaliauskas NA, Laurino K, Barbarich-Marsteller NC. 2014. alpha4betadelta-GABAARs in the hippocampal CA1 as a biomarker for resilience to activity-based anorexia. *Neuroscience.* 265:108–123.
- Arcelus J, Mitchell AJ, Wales J, Nielsen S. 2011. Mortality rates in patients with anorexia nervosa and other eating disorders. A meta-analysis of 36 studies. *Arch Gen Psychiatry.* 68:724–731.
- Atwood HL, Wojtowicz JM. 1999. Silent synapses in neural plasticity: current evidence. *Learn Mem.* 6:542–571.
- Bekhat M, Neigh GN. 2018. Sex differences in the neuro-immune consequences of stress: focus on depression and anxiety. *Brain Behav Immun.* 67:1–12.
- Bekkers JM. 2005. Presynaptically silent GABA synapses in hippocampus. *J Neurosci.* 25:4031–4039.
- Birmingham CL, Su J, Hlynsky JA, Goldner EM, Gao M. 2005. The mortality rate from anorexia nervosa. *Int J Eat Disord.* 38:143–146.
- Boraska V, Franklin CS, Floyd JA, Thornton LM, Huckins LM, Southam L, Rayner NW, Tachmazidou I, Klump KL, Treasure J, et al. 2014. A genome-wide association study of anorexia nervosa. *Mol Psychiatry.* 19:1085–1094.
- Casey BJ, Jones RM, Levita L, Libby V, Pattwell SS, Ruberry EJ, Soliman F, Somerville LH. 2010. The storm and stress of adolescence: insights from human imaging and mouse genetics. *Dev Psychobiol.* 52:225–235.
- Casey BJ, Lee FS. 2015. Optimizing treatments for anxiety by age and genetics. *Ann N Y Acad Sci.* 1345:16–24.
- Chen YW, Actor-Engel H, Sherpa AD, Klingensmith L, Chowdhury TG, Aoki C. 2017. NR2A- and NR2B-NMDA receptors and drebrin within postsynaptic spines of the hippocampus correlate with hunger-evoked exercise. *Brain Struct Funct.* 222:2271–2294.
- Chen CC, Lu J, Yang R, Ding JB, Zuo Y. 2017. Selective activation of parvalbumin interneurons prevents stress-induced synapse loss and perceptual defects. *Mol Psychiatry.* 23(7):1614–1625.
- Chen YW, Surgent O, Rana BS, Lee F, Aoki C. 2017. Variant BDNF-Val66Met polymorphism is associated with layer-specific alterations in GABAergic innervation of pyramidal neurons, elevated anxiety and reduced vulnerability of adolescent male mice to activity-based anorexia. *Cereb Cortex.* 27:3980–3993.
- Chen YW, Wable GS, Chowdhury TG, Aoki C. 2016. Enlargement of axo-somatic contacts formed by GAD-immunoreactive axon terminals onto layer V pyramidal neurons in the medial prefrontal cortex of adolescent female mice is associated with suppression of food restriction-evoked hyperactivity and resilience to activity-based anorexia. *Cereb Cortex.* 26:2574–2589.
- Chowdhury TG, Barbarich-Marsteller NC, Chan TE, Aoki C. 2014. Activity-based anorexia has differential effects on apical dendritic branching in dorsal and ventral hippocampal CA1. *Brain Struct Funct.* 219:1935–1945.
- Chowdhury TG, Rios MB, Chan TE, Cassataro DS, Barbarich-Marsteller NC, Aoki C. 2014. Activity-based anorexia during adolescence disrupts normal development of the CA1 pyramidal cells in the ventral hippocampus of female rats. *Hippocampus.* 24:1421–1429.
- Chowdhury TG, Wable GS, Sabaliauskas NA, Aoki C. 2013. Adolescent female C57BL/6 mice with vulnerability to activity-based anorexia exhibit weak inhibitory input onto hippocampal CA1 pyramidal cells. *Neuroscience.* 241:250–267.
- Eyre MD, Renzi M, Farrant M, Nusser Z. 2012. Setting the time course of inhibitory synaptic currents by mixing multiple GABA(A) receptor alpha subunit isoforms. *J Neurosci.* 32:5853–5867.

- Feldman ML. 1984. Morphology of the neocortical pyramidal neuron. New York: Plenum Press.
- Goldstein PA, Elsen FP, Ying SW, Ferguson C, Homanics GE, Harrison NL. 2002. Prolongation of hippocampal miniature inhibitory postsynaptic currents in mice lacking the GABA (A) receptor alpha1 subunit. *J Neurophysiol.* 88:3208–3217.
- Hirsch JC, Agassandian C, Merchan-Perez A, Ben-Ari Y, DeFelipe J, Esclapez M, Bernard C. 1999. Deficit of quantal release of GABA in experimental models of temporal lobe epilepsy. *Nat Neurosci.* 2:499–500.
- Horikawa K, Armstrong WE. 1988. A versatile means of intracellular labeling: injection of biocytin and its detection with avidin conjugates. *J Neurosci Methods.* 25:1–11.
- Huttunen P, Myers RD. 1986. Tetrahydro-beta-carboline micro-injected into the hippocampus induces an anxiety-like state in the rat. *Pharmacol Biochem Behav.* 24:1733–1738.
- Jiao Y, Zhang Z, Zhang C, Wang X, Sakata K, Lu B, Sun QQ. 2011. A key mechanism underlying sensory experience-dependent maturation of neocortical GABAergic circuits in vivo. *Proc Natl Acad Sci USA.* 108:12131–12136.
- Kataoka Y, Shibata K, Miyazaki A, Inoue Y, Tominaga K, Koizumi S, Ueki S, Niwa M. 1991. Involvement of the dorsal hippocampus in mediation of the antianxiety action of tandospirone, a 5-hydroxytryptamine1A agonistic anxiolytic. *Neuropharmacology.* 30:475–480.
- Kaye WH, Fudge JL, Paulus M. 2009. New insights into symptoms and neurocircuit function of anorexia nervosa. *Nat Rev Neurosci.* 10:573–584.
- Kinzig KP, Hargrave SL. 2010. Adolescent activity-based anorexia increases anxiety-like behavior in adulthood. *Physiol Behav.* 101:269–276.
- Liang J, Cagetti E, Olsen RW, Spigelman I. 2004. Altered pharmacology of synaptic and extrasynaptic GABAA receptors on CA1 hippocampal neurons is consistent with subunit changes in a model of alcohol withdrawal and dependence. *J Pharmacol Exp Ther.* 310:1234–1245.
- Mangan PS, Sun C, Carpenter M, Goodkin HP, Sieghart W, Kapur J. 2005. Cultured hippocampal pyramidal neurons express two kinds of GABAA receptors. *Mol Pharmacol.* 67:775–788.
- Marty S, Carroll P, Cellerino A, Castren E, Staiger V, Thoenen H, Lindholm D. 1996. Brain-derived neurotrophic factor promotes the differentiation of various hippocampal nonpyramidal neurons, including Cajal-Retzius cells, in organotypic slice cultures. *J Neurosci.* 16:675–687.
- McEwen BS, Bowles NP, Gray JD, Hill MN, Hunter RG, Karatsoreos IN, Nasca C. 2015. Mechanisms of stress in the brain. *Nat Neurosci.* 18:1353–1363.
- Mills KL, Goddings AL, Clasen LS, Giedd JN, Blakemore SJ. 2014. The developmental mismatch in structural brain maturation during adolescence. *Dev Neurosci.* 36:147–160.
- Mizoguchi Y, Ishibashi H, Nabekura J. 2003. The action of BDNF on GABA(A) currents changes from potentiating to suppressing during maturation of rat hippocampal CA1 pyramidal neurons. *J Physiol.* 548:703–709.
- Mizuno K, Carnahan J, Nawa H. 1994. Brain-derived neurotrophic factor promotes differentiation of striatal GABAergic neurons. *Dev Biol.* 165:243–256.
- Motulsky HJ, Brown RE. 2006. Detecting outliers when fitting data with nonlinear regression—a new method based on robust nonlinear regression and the false discovery rate. *BMC Bioinformatics.* 7:1–20.
- Nedelescu H, Chowdhury TG, Wable GS, Arbuthnott G, Aoki C. 2017. Cerebellar sub-divisions differ in exercise-induced plasticity of noradrenergic axons and in their association with resilience to activity-based anorexia. *Brain Struct Funct.* 222(1):317–339.
- Nielsen S, Moller-Madsen S, Isager T, Jorgensen J, Pagsberg K, Theander S. 1998. Standardized mortality in eating disorders—a quantitative summary of previously published and new evidence. *J Psychosom Res.* 44:413–434.
- Nusser Z, Sieghart W, Somogyi P. 1998. Segregation of different GABAA receptors to synaptic and extrasynaptic membranes of cerebellar granule cells. *J Neurosci.* 18:1693–1703.
- Packer AM, Yuste R. 2011. Dense, unspecific connectivity of neocortical parvalbumin-positive interneurons: a canonical microcircuit for inhibition? *J Neurosci.* 31:13260–13271.
- Peters A, Palay SL, Webster HD. 1991. The fine structure of the nervous system: neurons and their supporting cells. 3rd ed. New York: Oxford University Press.
- Rendeiro C, Rhodes JS. 2018. A new perspective of the hippocampus in the origin of exercise-brain interactions. *Brain Struct Funct.* 223:2527–2545.
- Rizzoli SO, Betz WJ. 2004. The structural organization of the readily releasable pool of synaptic vesicles. *Science.* 303:2037–2039.
- Romeo RD. 2010. Adolescence: a central event in shaping stress reactivity. *Dev Psychobiol.* 52:244–253.
- Sarro EC, Kotak VC, Sanes DH, Aoki C. 2008. Hearing loss alters the subcellular distribution of presynaptic GAD and post-synaptic GABAA receptors in the auditory cortex. *Cereb Cortex.* 18:2855–2867.
- Saul ML, Helmreich DL, Rehman S, Fudge JL. 2015. Proliferating cells in the adolescent rat amygdala: characterization and response to stress. *Neuroscience.* 311:105–117.
- Schlandler M, Frotscher M. 1986. Non-pyramidal neurons in the guinea pig hippocampus. A combined Golgi-electron microscope study. *Anat Embryol (Berl).* 174:35–47.
- Shen H, Gong QH, Aoki C, Yuan M, Ruderman Y, Dattilo M, Williams K, Smith SS. 2007. Reversal of neurosteroid effects at alpha4beta2delta GABAA receptors triggers anxiety at puberty. *Nat Neurosci.* 10:469–477.
- Shen H, Sabaliauskas N, Sherpa A, Fenton AA, Stelzer A, Aoki C, Smith SS. 2010. A critical role for alpha4betadelta GABAA receptors in shaping learning deficits at puberty in mice. *Science.* 327:1515–1518.
- Smink FR, van Hoeken D, Hoek HW. 2013. Epidemiology, course, and outcome of eating disorders. *Curr Opin Psychiatry.* 26:543–548.
- Smith SS, Woolley CS. 2004. Cellular and molecular effects of steroid hormones on CNS excitability. *Cleve Clin J Med.* 71 (Suppl 2):S4–S10.
- Spear LP. 2000. The adolescent brain and age-related behavioral manifestations. *Neurosci Biobehav Rev.* 24:417–463.
- Steinhausen HC. 2002. The outcome of anorexia nervosa in the 20th century. *Am J Psychiatry.* 159:1284–1293.
- Sullivan PF. 1995. Mortality in anorexia nervosa. *Am J Psychiatry.* 152:1073–1074.
- Talaenko AN. 1993. The neurochemical profiles of the dorsal hippocampus and the antiaversive effects of anxiolytics in different models of anxiety in rats. *J Nerv Ment Dis.* 43:621–626.
- Tanaka K, Watase K, Manabe T, Yamada K, Watanabe M, Takahashi K, Iwama H, Nishikawa T, Ichihara N, Kikuchi T, et al. 1997. Epilepsy and exacerbation of brain injury in mice lacking the glutamate transporter GLT-1. *Science.* 276:1699–1702.

- Tyler WJ, Pozzo-Miller LD. 2001. BDNF enhances quantal neurotransmitter release and increases the number of docked vesicles at the active zones of hippocampal excitatory synapses. *J Neurosci.* 21:4249–4258.
- Wable GS, Barbarich-Marsteller NC, Chowdhury TG, Sabaliauskas NA, Farb CR, Aoki C. 2014. Excitatory synapses on dendritic shafts of the caudal basal amygdala exhibit elevated levels of GABAA receptor alpha4 subunits following the induction of activity-based anorexia. *Synapse.* 68: 1–15.
- Wable GS, Chen YW, Rashid S, Aoki C. 2015. Exogenous progesterone exacerbates running response of adolescent female mice to repeated food restriction stress by changing alpha4-GABAA receptor activity of hippocampal pyramidal cells. *Neuroscience.* 310:322–341.
- Wable GS, Min JY, Chen YW, Aoki C. 2015. Anxiety is correlated with running in adolescent female mice undergoing activity-based anorexia. *Behav Neurosci.* 129:170–182.
- Wei W, Zhang N, Peng Z, Houser CR, Mody I. 2003. Perisynaptic localization of delta subunit-containing GABA(A) receptors and their activation by GABA spillover in the mouse dentate gyrus. *J Neurosci.* 23:10650–10661.
- Zhu LJ, Liu MY, Li H, Liu X, Chen C, Han Z, Wu HY, Jing X, Zhou HH, Suh H, et al. 2014. The different roles of glucocorticoids in the hippocampus and hypothalamus in chronic stress-induced HPA axis hyperactivity. *PLoS One.* 9:e97689.